Thin-Walled Structures 70 (2013) 39–48

Contents lists available at SciVerse ScienceDirect

Thin-Walled Structures

journal homepage: www.elsevier.com/locate/tws

Instability of a cracked cylindrical shell reinforced by an elastic liner

Y.T. Kim [a,1], B. Haghpanah [a,1], R. Ghosh [a], H. Ali [b], A.M.S. Hamouda [c], A. Vaziri [a,*]

[a] Department of Mechanical and Industrial Engineering, Northeastern University, Boston, MA 02115, USA
[b] FM Global, Norwood, MA 02062, USA
[c] Mechanical and Industrial Engineering, Qatar University, Doha, Qatar

ARTICLE INFO

Article history:
Received 6 February 2013
Received in revised form
18 April 2013
Accepted 18 April 2013

Keywords:
Buckling
Eigenvalue analysis
Cracked cylindrical shells
Elastic liners
Finite element method

ABSTRACT

Elastic liners are used for in situ repair and retrofitting of pipes as a cost effective alternative to the replacement of damaged parts and sections. In this paper, we studied the role of an elastic liner on the buckling behavior of a cracked cylindrical shell using finite element method. A special meshing scheme that could mimic the stress singularity at the crack tip was employed to model the cracked shells. Linear eigenvalue analysis was carried out to study the effect of crack geometry (length and orientation) as well as the material properties and thickness of the elastic liner on the buckling load and buckling shape of the cylindrical shell. We considered a combination of axial compression and internal pressure which is a typical loading for pipelines and pressurized liquid-retaining structures. Our results show that cracked shell's strength and mode of buckling for different crack length and orientations can be largely influenced by thickness and relative stiffness of the liner layer. In particular we report a gradual transition from local to global instability due to these size and orientation effects. Finally, the role of internal pressure on structural stability and local buckling of cracked shells, which strongly depends on the crack orientation and liner thickness, is discussed.

1. Introduction

Thin-walled shells are widely employed in pipelines, air- and space-crafts, marine structures, large dams, shell roofs, liquid-retaining structures and cooling towers [1,2]. In light of such widespread practical applications, it is important to investigate the failure behavior of these structures in order to compute safe envelopes of operations. Due to slenderness of their structure, buckling failure is one of the most common modes of failure. Presence of defects, particularly cracks in thin-walled structures may severely decrease their resistance to buckling and undermine structural stability [3–24]. When crack-induced damage is deemed sufficient to either compromise the structure load bearing capacity or make collapse imminent, the structural integrity must be restored to continue operation. The most direct approach to restore the load carrying capacity of a typical cracked structure is of course to replace the damaged component. However, this approach is often prohibitively expensive and worse, in many cases difficult to execute due to difficulty in physically accessing the damaged components. In addition, this procedure often leads to prolonged interruption in the service and usability of the structure, imposing additional operating costs.

In light of the above mentioned difficulties, alternative approaches have been proposed in recent years for retrofitting the damaged thin-walled structures by repairing and/or strengthening the shell structure wall in the damaged region using supportive liners. These in situ repair techniques are generally based on methods which provide engagement between the inserted liner and the existing pipe. Although such reinforcements seem to intuitively suggest strengthening of the structure against buckling, a systematic investigation of the mechanics of such reinforcements is necessary to make accurate prognosis as well as quantifiable design recommendations. In the current work, we address the elastic stability issue of a typical reinforced cracked shell structure through a finite element (FE) based numerical approach. A brief discussion on the pertinent literature in this area follows.

Elastic stability of thin walled cracked un-reinforced shells has been a subject of considerable academic scrutiny in the past. Earlier, El Naschie [25] focused on the buckling of circular cylindrical shells with a circumferential crack. The buckling load of these cracked shells is shown to be half of that of a corresponding pristine cylinder. Thereafter, notable theoretical analysis of stability was undertaken by Dyshel [26] who investigated the local instability issues of a circumferentially cracked shell under tensile loading by assuming infinitely long linear elastic, homogeneous cylinder with a shallow shell approximation to simplify the governing differential equations. Complex analysis was then used followed by the collocation method to obtain numerical solutions. Although the calculations are rigorous, they are somewhat tedious

* Corresponding author. Tel.: +1 6172706813.
E-mail addresses: vaziri@coe.neu.edu, avaziri2@gmail.com (A. Vaziri).
[1] Contributed equally to this work.

0263-8231/$ - see front matter © 2013 Elsevier Ltd. All rights reserved.
http://dx.doi.org/10.1016/j.tws.2013.04.008

even for this simplified case and can become intractable when applied to more realistic highly curved, layered or composite structures. These computational difficulties motivated an increasing focus towards more extensive numerical methods such as the FE based approaches. Estekanchi and Vafai [9] developed a computational model to address the specific FE meshing issues stemming from the presence of a crack on the shell surface. The development of this model greatly aided extensive FE based parametric studies of cracked shells wherein critical defect parameters such as crack length and orientation could be conveniently and accurately varied. They utilized this meshing scheme to carry out FE based bifurcation analysis for a variety of crack sizes and orientations on unreinforced cylindrical shells under axial tension and compression loading. In particular they reported that the buckling mode of a cylindrical shell with a circumferential crack changes with crack length. The reduction of the load carrying capacity of the structure due to the crack was expressed in terms of an analytical expression based on the extensive parametric analysis carried out by the authors. More recently Vaziri and Estekanchi [27] utilized the above mentioned meshing scheme to investigate the behavior of cracked cylindrical shells under combined internal pressure and axial compression. They considered through and thumbnail cracks. The effect of crack orientation and internal pressure on the buckling behavior of cracked shells without elastic liners was studied. Their results showed that depending on the length, orientation and the internal pressure, local buckling may precede the global buckling of the cylindrical shell. In general, internal pressure increases the buckling load associated with the global buckling mode while for the local buckling modes, the effect of internal pressure depends critically on the crack orientation. This analysis was further extended to study the buckling behavior of composite shells by Vaziri [28]. The study clearly indicated the role of material anisotropy can be utilized to minimize the reduction in load bearing capacity of the structure. These above mentioned FE based approaches were further extended by Haghpanah et al. to study the buckling behavior of cracked cylinders with multiple parallel cracks [29]. In their study the authors reported the existence of a minimum cutoff interaction distance between cracks beyond which they do not affect the buckling load.

These FE based investigations have clearly been successful in addressing a host of issues not possible through analytical or semi-analytical techniques. These FE models enable us to carry out systematic and detailed numerical simulations of these structures over a broad range of geometrical parameters and loading conditions. This provides better insights into the structural performance of cracked shells and allows identification of critical crack and defect geometries as well as loading conditions that are most detrimental to the performance of the system. It is noteworthy that the previously discussed body of research did not address the additional mechanical effects brought in by the reinforcing liner used to repair damaged cylindrical structures. In this paper, we study the buckling instability of cracked cylindrical shells with an elastic liner, that resembles the configuration of a typical damaged pipe retrofitted using a typical commercially available liner. The loading condition considered is a combination of axial compression and internal pressure, which is the most common loading condition in pipelines, liquid-retaining structures, and also often in aerospace and marine structures. Detailed numerical simulations are performed to study the effect of liner relative thickness and stiffness on the overall buckling behavior of reinforced cracked cylindrical shell. The role of crack length and orientation, as well the effect of internal pressure on buckling behavior of the crack cylindrical shells were studied.

The paper is organized as follows. We develop the computational model in Section 2; firstly a normalization scheme based on buckling behavior of pristine uncracked shells is introduced. We devote the next subsection to build the finite element model for the cracked cylindrical shells with various crack lengths and orientations using the meshing scheme proposed by Estekanchi and Vafai [9]. This method accurately captures the crack-tip stress intensity factor with relatively few elements and simplifies the generation of numerical models of cracked shells enabling us to run a comprehensive parametric study on the behavior of cracked shells. Next, in Section 3 we discuss the results concerning buckling loads under uniaxial compression over a wide range of crack size and orientation, and for different reinforcement properties. Thereafter we highlight the effect of internal pressure on the buckling behavior of cracked reinforced structure. Conclusions follow in Section 4.

2. Computational model

In this section, the essential components of the computational model which will be used to simulate the buckling behavior of the cracked cylindrical shell are presented. To this end, first we describe a normalization scheme for analyzing the numerical simulation results and then the finite element (FE) model which will be used to obtain the numerical results.

2.1. Normalization using buckling behavior of uncracked bi-layer cylindrical shell

In this work, in addition to geometrical parameters such as radius and thickness of the cylinder as well as material parameter like elastic modulus, we selected the theoretical buckling load of a geometrically analogous uncracked shell F_{th} the normalizing parameter. Thus, we use the ratio of FE calculated critical buckling load of the cracked cylinder F_c to F_{th} as a natural non-dimensional parameter for this problem. We call this parameter the normalized buckling load $\gamma = F_c/F_{th}$ and its derivation is explained below.

We note that analytical and semi-analytical calculation of critical buckling load for single layered cylindrical shells is a classical problem [30]. In addition, the extended problem of stability of multilayered shells have been traditionally analyzed in the context of anisotropic laminate and fiber reinforced composites, functionally graded materials under mechanical loading [31] and bi-metallic shells under thermo-mechanical loading [32]. For clarity, the derivation of buckling load and buckling behavior of an isotropic liner-reinforced cylindrical shell under purely mechanical compressive force is briefly explained below.

We start by assuming that the buckling shape of the bi-layer cylinder is in the form of axisymmetrical sinusoidal pattern observed in the buckling of long uniform cylinders under axial compression. The reinforced cylindrical shell is modeled as an elastic isotropic bi-layer lamina, with the two layers having different elastic moduli and same Poisson's ratio. The thickness and elastic modulus of the outer metallic shell and inner polymeric liner are denoted by t, E and t_p, E_p respectively. The radius of the cylinder, defined as the distance between center and the neutral surface, is denoted by R (see Fig. 1A).

At each shell cross section, the axes x, y and z are oriented along the longitudinal, tangential and radial direction of the cylinder, respectively, with their origin on the neutral surface. We consider an element cut out of the composite lamina by two pairs of planes parallel to the xz and yz planes as shown in Fig. 1(B). The bending neutral surface in the shell–liner lamina can be determined by loading the composite layer to pure uniaxial bending. Under this loading, planes perpendicular to neutral surface are assumed to remain planar and perpendicular to the neutral surface even after deformation. Under pure bending, the requirement of zero axial

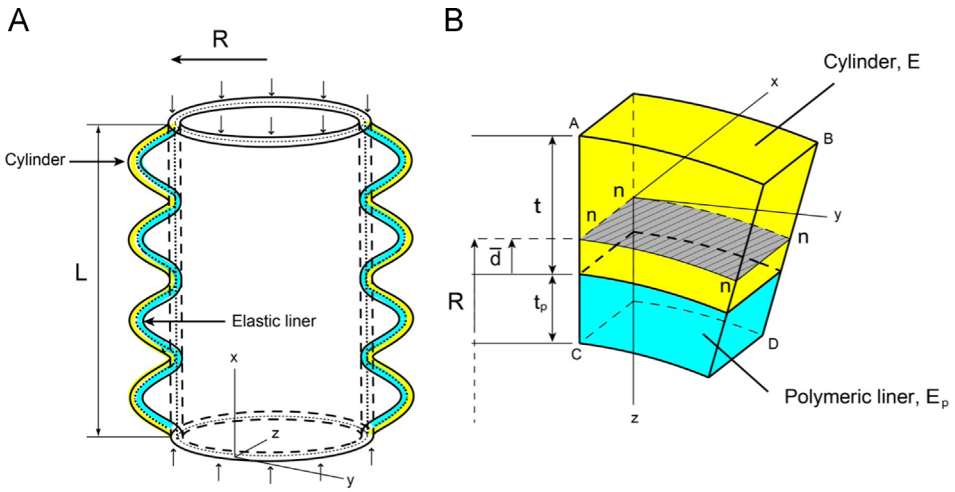

Fig. 1. (A) Axisymmetrical buckling mode shape of a cylindrical shell with an elastic liner under axial compression. (B) The element cut out of the cylindrical shell by two pairs of planes parallel to the *xy* and *yz* planes.

force allows us to calculate the distance $\bar{d}$ (positive outward) of the neutral surface from the shell–liner interface:

$$\bar{d} = \frac{(t/2)Et + (-t_p/2)E_p t_p}{Et + E_p t_p} = \frac{t}{2}\left(\frac{1-(t_p/t)^2(E_p/E)}{1+(t_p/t)(E_p/E)}\right) \tag{1}$$

Now, let the curvatures of the neutral surface in sections parallel to the *zx* and *yz* planes be $\chi_x = 1/\rho_x = -\partial^2 w/\partial x^2$ and $\chi_y = 1/\rho_y = -\partial^2 w/\partial y^2$, respectively, with positive curvature corresponding to bending which is convex down and w denoting the deflection of the plate. Then, the unit elongations in the x and y directions of an elemental lamina at *zdistance from the neutral surface* can be found as $\varepsilon_x = z/\rho_x$ and $\varepsilon_y = z/\rho_y$. From Hooke's law the corresponding x and y normal stresses are $\sigma_x = E(z)(z(1/\rho_x) + \nu(1/\rho_y))/(1-\nu^2)$ and $\sigma_y = E(z)z((1/\rho_y) + \nu(1/\rho_x))/(1-\nu^2)$, where$\nu$ is Poission's ratio of both shell and liner and $E(z)$ is Young's modulus at distance z. The bending moment per unit length of the edges parallel to the y-axis, denoted by M_x, can be expressed as

$$M_x = \int_{-t_p-\bar{d}}^{t-\bar{d}} z\sigma_y dz = \int_{-t_p-\bar{d}}^{t-\bar{d}} E(z)z^2\left(\frac{1}{\rho_y} + \nu\frac{1}{\rho_x}\right)/(1-\nu^2)dz$$

$$= D\left(\frac{1}{\rho_x} + \nu\frac{1}{\rho_y}\right) \tag{2}$$

and similarly for M_y

$$M_y = \int_{-t_p-\bar{d}}^{t-\bar{d}} z\sigma_x\, dz = \int_{-t_p-\bar{d}}^{t-\bar{d}} E(z)z^2\left(\frac{1}{\rho_x} + \nu\frac{1}{\rho_y}\right)/(1-\nu^2)dz$$

$$= D\left(\frac{1}{\rho_y} + \nu\frac{1}{\rho_x}\right) \tag{3}$$

where D is the flexural rigidity of the lamina given by

$$D = \int_{-t_p-\bar{d}}^{-\bar{d}} E_p z^2/(1-\nu^2)dz + \int_{-\bar{d}}^{t-\bar{d}} Ez^2/(1-\nu^2)dz$$

$$= (EI^0 + E_p I_p^0)/(1-\nu^2) \tag{4}$$

here $I^0 = \int_{-\bar{d}}^{t-\bar{d}} z^2\, dz$, $I_p^0 = \int_{-t_p-\bar{d}}^{-\bar{d}} z^2\, dz$ denote the second moment of area of the shell and liner cross sections around the neutral axis (superscript 0 denotes the values are measured from the neutral axis of the shell–liner compound layer).

Similarly, the resultant forces acting in the neutral surface of the shell can be obtained as

$$N_x = \int_{-t_p-\bar{d}}^{t-\bar{d}} \sigma_x\, dz = (Et + E_p t_p)\frac{\varepsilon_1 + \nu\varepsilon_2}{1-\nu^2}$$

$$N_y = \int_{-t_p-\bar{d}}^{t-\bar{d}} \sigma_y\, dz = (Et + E_p t_p)\frac{\varepsilon_2 + \nu\varepsilon_1}{1-\nu^2}$$

$$N_{xy} = \int_{-t_p-\bar{d}}^{t-\bar{d}} \tau_{xy}\, dz = (Et + E_p t_p)\frac{\gamma}{2(1+\nu)} \tag{5}$$

where ε_1, ε_2 and γ_{12} (not to be confused with the non-dimensional buckling load γ introduced earlier) are the x, y normal and xy shearing strains of the neutral surface respectively.

The strain energy in an element of the lamina due to $M_x\, dy$ and $M_y\, dx$ bending moments and $M_{xy}\, dx$ and $M_{xy}\, dy$ twist moments can be calculated as the product of the components of moment and the angle between the sides of the element after bending. The total bending work in the lamina is obtained by integrating the strain energy over the thickness of the lamina [30]

$$U_b = 1/2D \int\int \left\{\left(\frac{\partial^2 w}{\partial x^2} + \frac{\partial^2 w}{\partial y^2}\right)^2 - 2(1-\nu)\left[\frac{\partial^2 w}{\partial x^2}\frac{\partial^2 w}{\partial y^2} - \left(\frac{\partial^2 w}{\partial x \partial y}\right)^2\right]\right\} dx\, dy \tag{6}$$

Also the stretching (membrane) energy due to stretching of the neutral surface in the lamina is $U_s = \iint \frac{1}{2}(N_x\varepsilon_1 + N_y\varepsilon_2 + N_{xy}\gamma)dA$. Substituting from Eq. (5), the stretching energy can be obtained as [30]

$$U_s = \frac{(Et + E_p t_p)}{2(1-\nu^2)} \int\int (\varepsilon_1 + \varepsilon_2)^2 - 2(1-\nu)(\varepsilon_1\varepsilon_2 - \frac{1}{4}\gamma_{12}^2)]dx\, dy \tag{7}$$

The total energy of deformation is obtained by adding together expressions (6) and (7). Similar to buckling of uniform cylindrical shells under axial compression, the cylindrical shell with elastic liner is assumed to buckle axisymmetrically under axial compression (see Fig. 1A). Assuming an axisymmetric buckling deformation, the radial displacement of the cylinder during buckling to be $w = -A\sin(m\pi x/l)$ with a buckling wavelength $2l/m$, the x curvature of the deformed lamina would be $\chi_x = -\partial^2 w/\partial x^2 = -A(m^2\pi^2/l^2)\sin(m\pi x/l)$ and the y curvature and xy twist of the lamina are zero ($\gamma_{12} = \chi_y = \chi_{xy}$). The increase of strain energy during buckling, $\Delta U = \Delta U_s + \Delta U_b$, can be found from

Eqs. (6) and (7) as

$$\Delta U = -2\pi(Et + E_p t_p)v\varepsilon_0 \int_0^l A \sin\frac{m\pi x}{l}\,dx + \frac{\pi A^2(Et + E_p t_p)l}{2R} + A^2\frac{\pi^4 m^4}{2l^4}\pi RlD \tag{8}$$

where ε_0 denotes the axial strain before buckling, $\varepsilon_0 = -N_{cr}/(Et + E_p t_p)$, and N_{cr} denotes the critical value of compressive force per unit length. The work done by compressive forces during buckling can be obtained as amount of axial force, $F = 2\pi a N_{cr}$, times the amount of axial shrinkage of the neutral surface, which can be estimated from $\Delta x = \frac{1}{2}\int_0^l \left[(dw/dx)^2 - v(w/a)\right]dx$. This yields [30]

$$\Delta T = 2\pi N_{cr}\left(v\int_0^l A \sin\frac{m\pi x}{l}\,dx + \frac{R}{4}A^2\frac{m^2\pi^2}{l}\,dx\right) \tag{9}$$

Equating expressions (8) and (9), we obtain

$$N_{cr} = D\left(\frac{m^2\pi^2}{l^2} + \frac{Et + E_p t_p}{R^2 D}\frac{l^2}{m^2\pi^2}\right) \tag{10}$$

The minimum value of the above expression occurs at $m\pi/l = \sqrt[4]{(Et + E_p t_p)/(R^2 D)}$ with buckling wavelength $\Gamma = 2\pi\sqrt[4]{R^2 D/(Et + E_p t_p)}$. The associated buckling force of the bi-layer cylinder is obtained as

$$F_{th} = 2\pi R N_{cr} = 4\pi\sqrt{(Et + E_p t_p)D} \tag{11}$$

Substituting from Eq. (4), the theoretical buckling load of a bi-layer elastic cylinder is obtained as $F_{th} = F_{th}^s \sqrt{(1 + (E_p t_p/Et))(1 + (E_p t_p^3/Et^3)) + 3(1 + (t_p/t))^2 (E_p t_p/Et)}$, where $F_{th}^s = 2\pi/\sqrt{3(1-\nu^2)}Et^2$ is the classical buckling load of a long single-layered unflawed cylindrical shell under axial compression. Fig. 2 (A) graphically shows the normalized buckling load contours of the reinforced cylindrical shell, defined as $\overline{F}_{th} = F_{th}/F_{th}^s$, as a function of thickness ratio, t_p/t, and stiffness ratio, E_p/E, of polymeric layer to cylindrical shell. The incremental gain in buckling load is increased remarkably as the thickness as well as stiffness of the liner increases. Fig. 2B displays the wavelength contours of a cylindrical shell with liner, plotted for different values of thickness ratio, t_p/t, and stiffness ratio, E_p/E, of the elastic liner to the cylindrical shell. The results are presented in a non-dimensional form, $\overline{\Gamma}$, where the buckling wavelength of the reinforced cylinder is normalized by the buckling wavelength of the counterpart cylindrical shell with no elastic liner reinforcement. This completes our analytical treatment of uncracked bi-layer cylinders.

2.2. Finite element model of the cracked cylinders

In this subsection, we describe the FE based numerical model of bilayer cracked cylindrical shells. The cracked cylinder considered has a length of $L = 2$ m, radius $R = 0.2$ m and a thickness of $t = 1.2$ mm. The shell is meshed using the meshing scheme discussed before by Estekanchi and Vafai [9]. In this mesh zooming technique, the FE mesh is uniform far from the crack tip and gets progressively refined in the crack tip area (see Fig. 2). The zooming level in this scheme denotes the number of element layers surrounding the crack tip with reduced element size compared to the uniform element size in the uncracked region. The zooming factor denotes the relative size (both length and width) of the element at each element layer to the size of the element in the previous element layer as approaching the crack tip. For meshing the crack region, the zooming factor of 1/2 and zooming level of 6 were used. This zooming factor results in the crack tip element size 1/64 of the element size far from the crack tip. The cylindrical shell in the uncracked region was meshed into 150 elements in each of the axial and circumferential directions. Fig. 3 shows examples of the FE mesh for circumferentially and longitudinally cracked cylinders developed based on this meshing scheme. This meshing scheme captures the singularity of stresses in the crack tip region with high fidelity, while simultaneously allowing creation of many models with various crack length and orientation required for parametric studies and reducing the computational complexity. Shells with different crack lengths, a, and crack orientations, α – where $\alpha = 0$ denotes the circumferential direction – were meshed using a MATLAB based code and imported into Abaqus, a commercially available FE software. The elastic liner was modeled as an uncracked cylindrical shell of the same radius and length as the cracked cylindrical shell. The size of the element for meshing the cylindrical shell that represents the elastic liner was uniform and equivalent to the element size of the cracked shell far from the crack tip of the outer shell. Both the shell and elastic liner were modeled using eight-node shell elements (S8R) with reduced integration and quadratic shape functions. Mesh sensitivity analysis

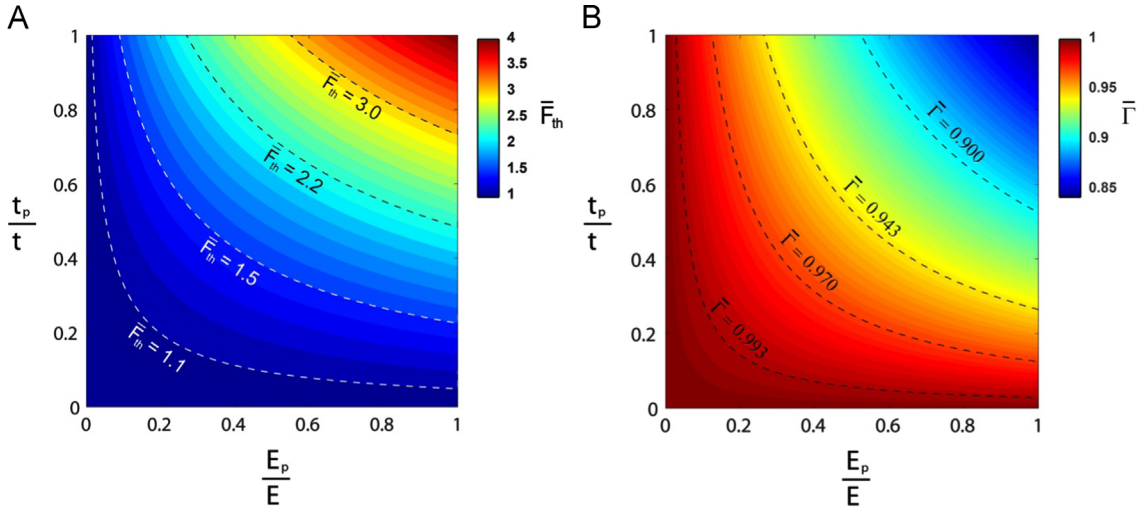

Fig. 2. (A) Buckling load of a perfect cylindrical shell with polymeric liner normalized by the buckling load of the cylinder without liner for different values of polymeric layer to cylindrical shell thickness and stiffness ratio. (B) Buckling wavelength of a perfect cylindrical shell with polymeric liner normalized by the buckling wavelength of the cylinder without liner for different values of polymeric layer to cylindrical shell thickness and stiffness ratio.

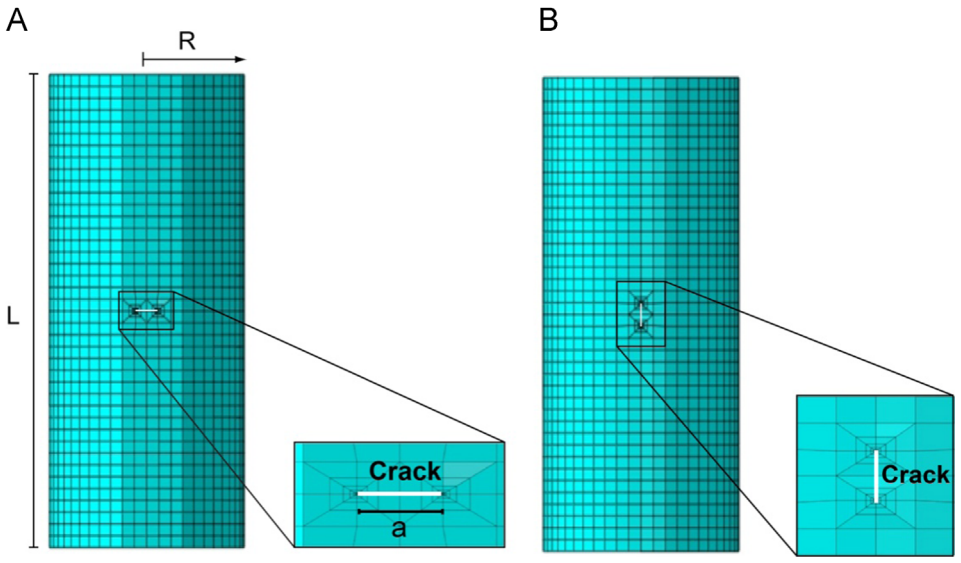

Fig. 3. Computational models of a cylindrical shell with (A) a circumferential crack and (B) a longitudinal crack developed by employing a special meshing scheme at the crack region, proposed by Estekanchi and Vafai [9].

was performed to verify that the results were independent of the mesh size.

Eigenvalue analysis using a linear eigenvalue solver was carried out to obtain the buckling load and mode shapes of the cracked cylindrical shells under combined axial compression and internal pressure. For the cracked shells, we assumed a linear isotropic elastic material with Young's modulus, $E=69$ GPa and Poisson's ratio, $\nu=0.35$ (typical properties for aluminum). For the elastic liner, we considered a wide range of liner material stiffness. It should be noted that during the repair process of damaged pipes, a liner with smaller diameter is inserted into the damaged section of the host pipe. A close-fit between the liner and the native shell structure is generally achieved by applying pressure and heat. This is modeled as a no-slip interface condition between the liner and shell and an axially fixed boundary condition at one end of the cylinder in our FE model.

3. Numerical results and discussions

In this section we describe the numerical results obtained from the simulation the FE based model developed above. We start by describing the buckling response of the cracked cylinder under pure axial compression and then proceed to describe the influence of internal pressure on the buckling behavior.

3.1. Cracked cylindrical shells with an elastic liner under axial compression

Depending on the buckling mode shape, we have defined three distinct deformation modes for the cracked reinforced shells: global buckling mode where cracked shell has approximately the same (within 95%) buckling load and similar mode shape as those of the intact composite cylinder; (b) transition mode with a crack which will affect both the buckling shape as well as the buckling load, but the buckling deformation is still global and not fully localized; (c) local mode with a localized buckling deformation close to the crack region and very low buckling load compared to the uncracked shell. Fig. 4A and B show the normalized buckling load of a reinforced cylindrical shell with a single circumferential crack ($\alpha=0^\circ$) and a longitudinal crack ($\alpha=90^\circ$), respectively obtained from our FE calculations for a reinforced cylindrical shells with $E_p/E=0.01$. The buckling loads are presented for a cracked cylindrical shell with different crack sizes, and reinforced with liners of different thickness ratio t_p/t. In Fig. 4A and B, we plot the dependence of normalized buckling load of the reinforced cylinder with normalized crack length for various liner thickness. The results suggest that sufficiently small cracks have no significant effect on the buckling behavior of a cylindrical shell, i.e. a global form of buckling occurs at $\gamma\approx1$ featuring axisymmetric corrugations with wavelength $\Gamma=2\pi\sqrt[4]{R^2D/(Et+E_pt_p)}$, where D is the flexural rigidity of the shell. However, for the shells with larger cracks, local buckling occurs and the buckling load of the shell decreases significantly. The results also indicate that reinforced shells with a thicker liner have higher value of γ for a prescribed crack length, and also the buckling strength of cylinders with longitudinal cracks is more severely compromised due to the presence of a crack of certain length compared to cylinders with circumferential cracks. In next set of results, we summarized the effect of relative stiffness of the elastic liner on the normalized buckling load of cracked cylindrical shells. Fig. 5(A) and (B) show the results for cylindrical shells with a circumferential and a longitudinal crack of length ratio $a/R=0.2$, respectively. Here, normalized buckling loads are plotted for different values of relative thickness as well as relative stiffness of the liner. The simulations indicate that increasing the relative stiffness increases the normalized buckling load and interestingly the buckling behavior of a cracked shell may even be restored by using a liner with appropriate thickness and stiffness. The buckling strength of cylinders with longitudinal cracks is more sensitive to liner material properties compared to cylinders with circumferential crack when $E_p/E\leq0.05$. Thus the reinforcement might be more effective for cylinders with longitudinal cracks. For reinforced shells with $E_p/E\leq0.05$, the normalized buckling load is significantly smaller for longitudinal cracks compared to the circumferential crack of same length (see Fig. 5A and B).

To further explore the effect of crack orientation, we have considered cylindrical shells with a crack of length $a/R=0.2$ and four different orientations $\alpha=0^\circ$, 30°, 60°, and 90°. The results are summarized in Fig. 6A. Maximum normalized buckling load was observed for cracks with $\alpha=30^\circ$ for lower value of E_p/E, as shown by the numerical simulations. Local buckling mode shapes for the case where $a/R=0.2$ and $E_p/E=0.1$ at four different angles

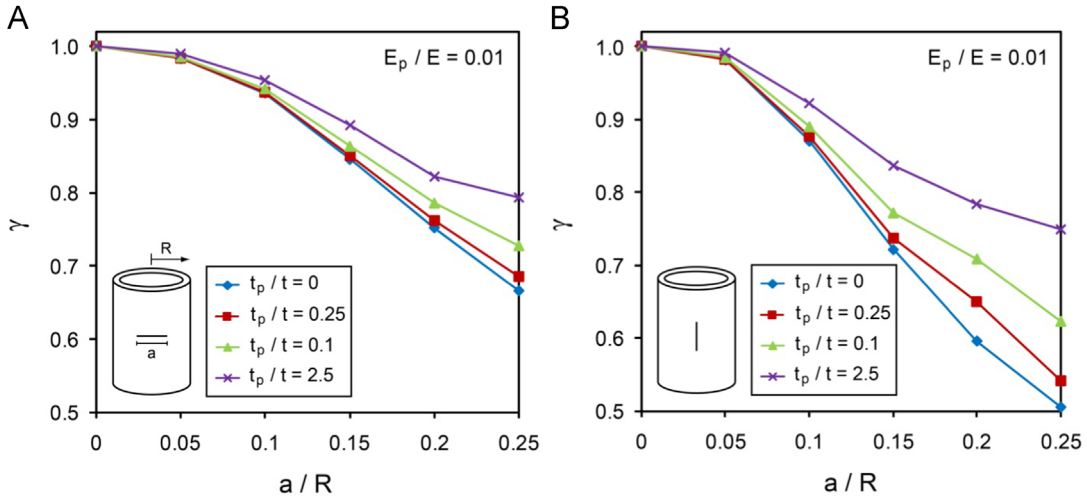

Fig. 4. Normalized buckling load (γ) of a reinforced cylindrical shell versus crack length ratio, (a/R) with a (A) circumferentially oriented crack ($\alpha=0^o$) and (B) longitudinally oriented crack ($\alpha=90^o$) for different liner to shell thickness ratios, (t_p/t). The elastic modulus ratio of the polymeric liner to the metallic shell is $E_p/E=0.01$ for both set of simulations.

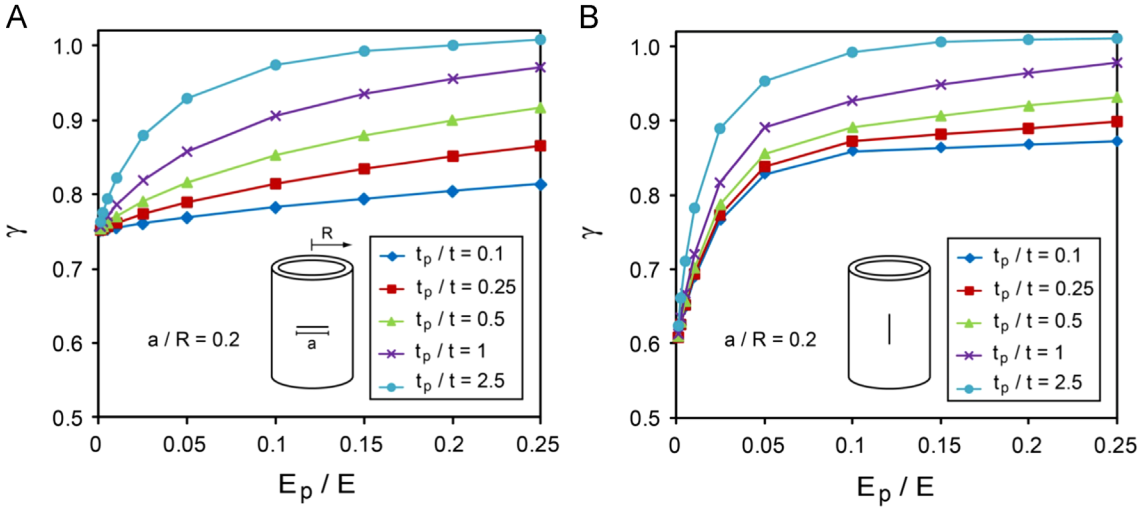

Fig. 5. Normalized buckling load versus liner to shell Young's modulus ratios, (E_p/E), for different liner to shell thickness ratios, (t_p/t) of a reinforced cylindrical shell with a (A) circumferential crack ($\alpha=0^o$) and (B) longitudinal crack ($\alpha=90^o$). The crack length to cylinders radius ratio is kept constant at $a/R=0.2$ for the simulations.

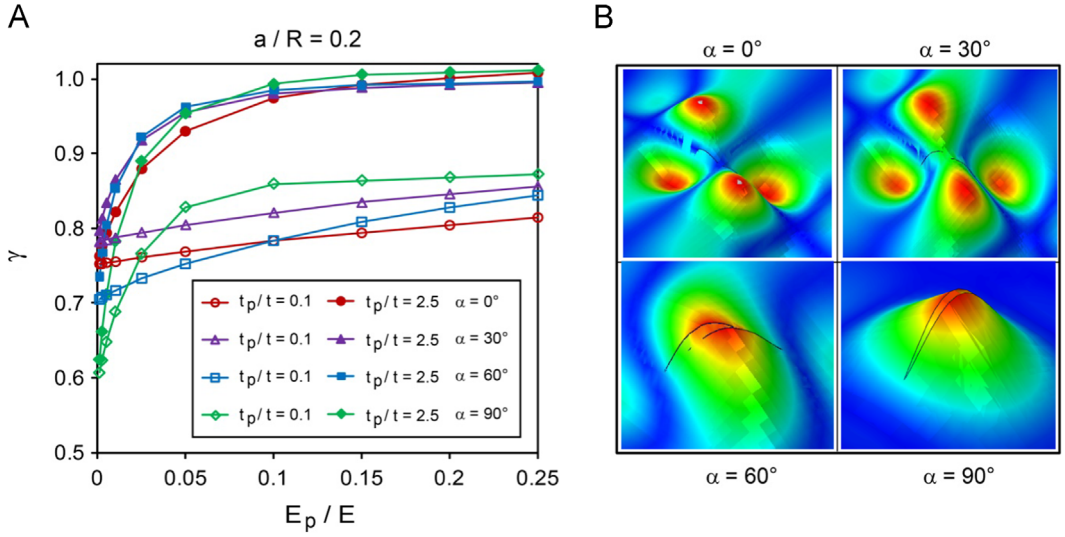

Fig. 6. (A) Normalized buckling load of a lined cylindrical shell versus E_p/E for different crack angles at $t_p/t=0.1$ and 2.5. (B) Local buckling shapes at the cracked region for four different crack orientations.

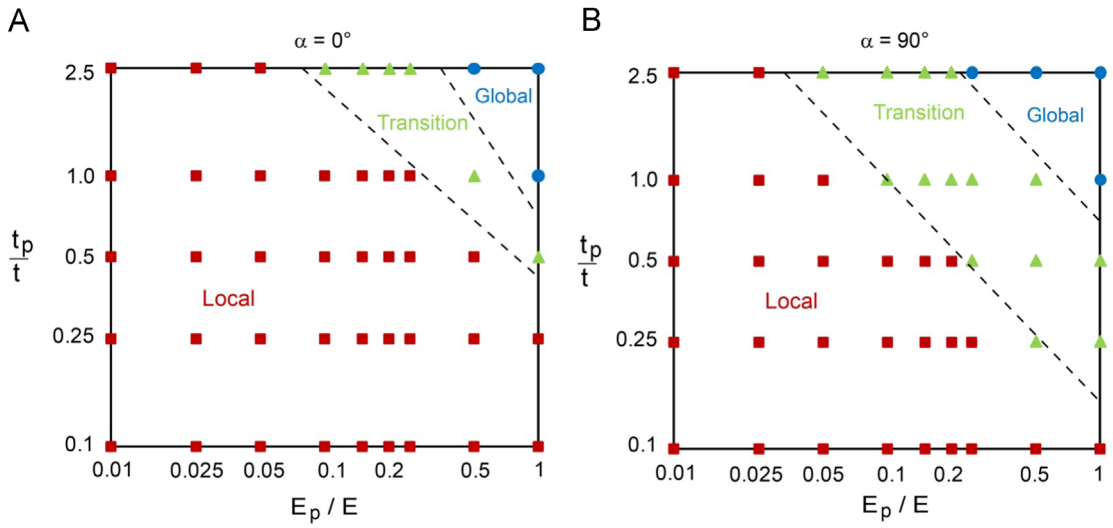

Fig. 7. The maps showing the dominance of global, transitional and local buckling shapes in a lined cylindrical shell with a (A) circumferential and (B) longitudinal crack based on Young's modulus ratio, (E_p/E), and the thickness ratio, (t_p/t).

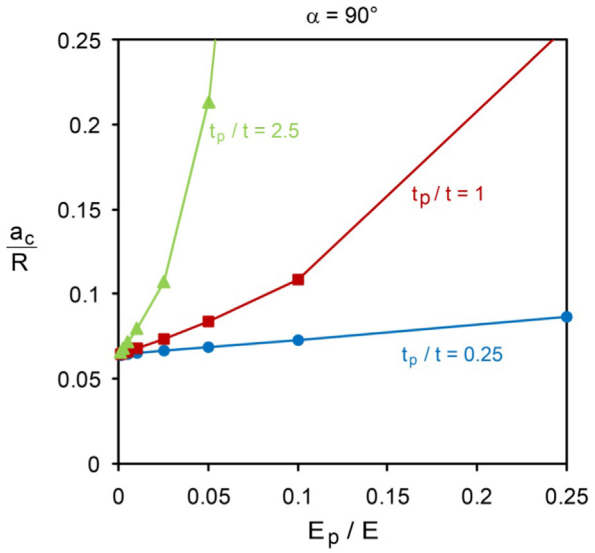

Fig. 8. Critical crack length ratio (a_c/R) versus Young's modulus ratio, (E_p/E), for different thickness ratios, (t_p/t).

are shown in Fig. 6B. For smaller values of α, buckling shapes are similar with maximum outward and inward displacements occurring at the crack tips and the deformation being approximately symmetric with respect to the crack. For greater values of α, the cracked cylinder bulges out symmetrically with respect to the crack axis which is why cracked cylindrical shells with bigger values of α are more sensitive to either relative thickness or relative stiffness of the liner. In Fig. 7, we provide maps for reinforced shells showing the dependence of buckling mode shapes on the relative thickness, relative stiffness, and the crack orientation. For identifying local, transition, and global shapes the associated buckling loads were examined. A local buckling for the cylinder was identified with a corresponding normalized buckling load in the range of $0.95 < \gamma < 1$. The transition and the global shapes of buckling were associated with normalized buckling loads in the ranges of $0.85 < \gamma < 0.95$ and $\gamma < 0.85$, respectively. The crack length to cylinders radius ratio is $a/R = 0.2$. By introducing a large enough crack, the buckling mode changes to local buckling mode. We can define a critical crack length at each orientation, a_c, as the maximum crack length leading to a global buckling shape. In Fig. 8, we have shown the dependence of the critical crack length on the relative stiffness as well as the relative thickness of the liner. The results suggest that a higher value of liner relative thickness leads to a larger value of critical crack length. Also, by increasing the relative stiffness the critical crack length increases.

In Fig. 9A and B we plot the normalized buckling loads versus the stretching stiffness ratio $E_p t_p/Et$ for five different elastic liner thicknesses. The crack length to cylinders radius ratio is $a/R = 0.2$. The broken lines represent trends of the normalized buckling load of the reinforced crack shell with different crack orientations. In Fig. 9A, the broken lines represent the trend from FE results of the crack orientations of 0° and 30°, respectively. In Fig. 9B, the broken lines represent the trend from FE results of the crack orientations of 0° and 60°, respectively. From both plots, it is clear that increasing the stretching modulus unambiguously improves the buckling load for all crack orientation. However, as the comparative plots of Fig. 8A and B show, a crack oriented at 60° although weakens the buckling characteristic more than a corresponding crack oriented at 0° or 30° results in a much faster recovery of strength when the stretching modulus of the liner is increased. Interestingly, when we plot the normalized buckling loads versus the stretching modulus for an axial (i.e. 90°) crack, the data points do not collapse into a single curve particularly at the lower end of the stretch modulus. This suggests that at lower values of membrane stretch modulus, the thickness ratio itself may be an important buckling parameter for an axial crack.

3.2. Role of internal pressure

The computational model is next used to study the effect of internal pressure on the first buckling mode due to axial compression of the cracked shell–elastic liner combination described earlier with different crack orientations. We define a normalized loading parameter, $\lambda = 2\pi R^2 P/F$, where P denotes the internal pressure applied to the inside surface of the elastic liner and F denotes the total axial force applied to the shell. The effect of the internal pressure on the normalized buckling load of cylindrical shells combined with an elastic liner for various crack orientations are depicted in Fig. 10. Fig. 10A shows the dependence of the normalized buckling loads of the circumferential cracked cylindrical shells reinforced with an elastic liner on the normalized loading parameter λ, for four different liner thickness, $t_p/t = 0$, 0.25, 1, and 2.5. The buckling modes of the elastic liner-reinforced cylindrical shells with a through circumferential crack show local

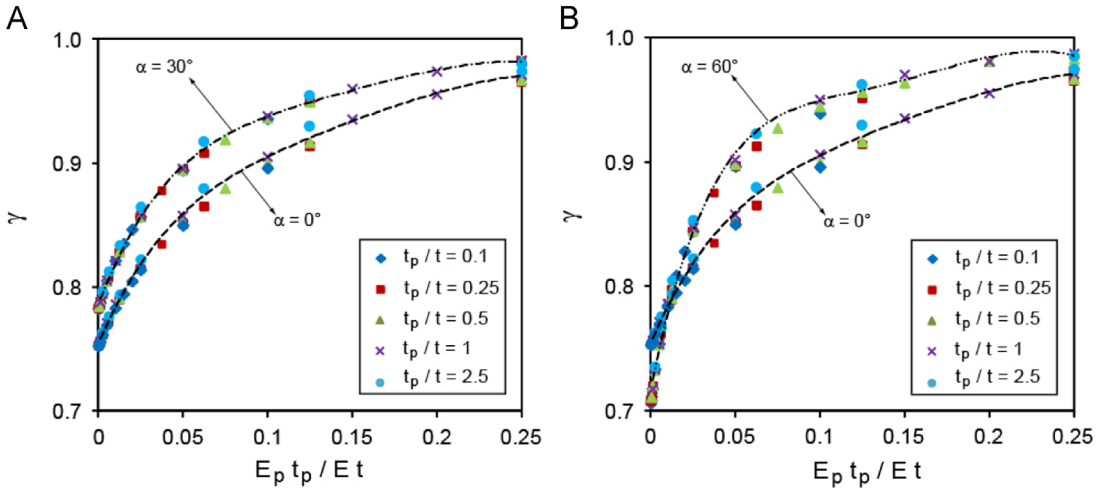

Fig. 9. (A) and (B) Normalized buckling loads versus normalized stretching stiffness of the reinforced cylindrical shell with a crack for different liner to cylindrical shell thickness ratios, (t_p/t), at the crack orientations of 0°, 30° (top left), 0°, 60° (top right).

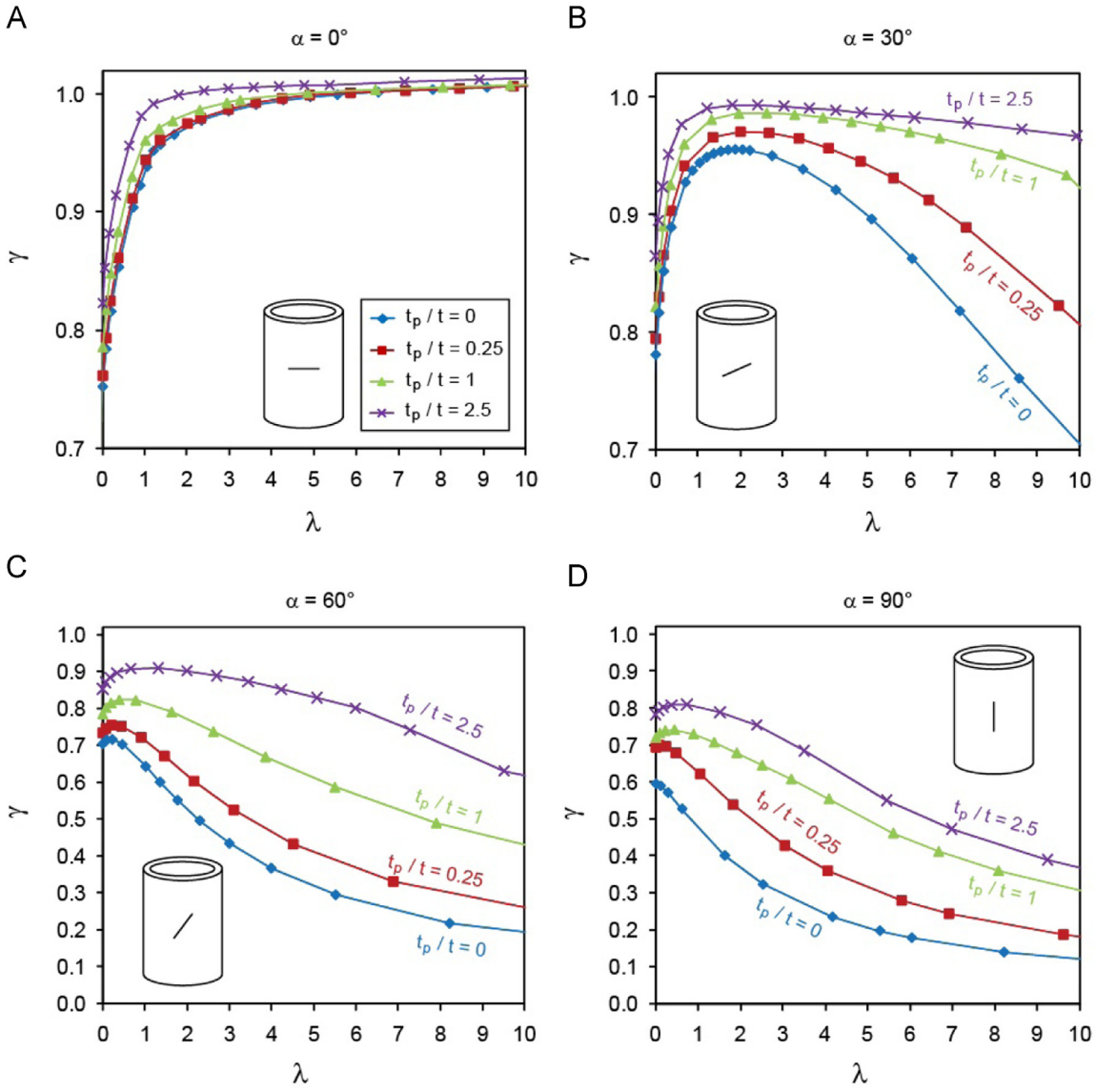

Fig. 10. (A)–(D) Normalized axial buckling load, γ, of a lined cracked cylindrical shell under uniform internal pressure versus the normalized loading parameter, λ, for different liner to shell thickness ratios, (t_p/t), at crack angles of α=0°, 30°, 60° and 90°.

buckling modes at the low internal pressure zone. For this case we also found that the buckling load associated with the first buckling mode sharply increased from the low internal pressure to high internal pressure region for all of elastic thickness ratios. This can be explained in terms of additional stiffening effect provided by the internal pressure acting on the underlying liner.

Next, we study the effect of crack angle on the buckling behavior of cracked cylindrical shells under combined internal pressure and axial compression for two crack angles: 30° and 60°. Fig. 10B and C depict the dependence of normalized buckling load on the normalized pressure loading parameter λ for crack angles 30° and 60°, respectively. We find that when the crack angle is 30°, the normalized buckling load rapidly increases in the low pressure regime. Thus, in this regime, the internal pressure helps to strengthen the buckling strength of the structure. However, quite interestingly, beyond a sufficiently high pressure load, the buckling strength sharply diminishes for both cases. For a crack angle of 30°, this inflection point was found to occur at normalized load value of $\lambda = \lambda_{cr} = 2$. This critical value of inflection is reached even earlier for cracks oriented at 60°. By the time the crack orientation becomes vertical (see Fig. 10D), this inflection almost disappears with $\lambda_{cr} \ll 1$. Thus we conclude that any beneficial effect of internal pressure on the buckling load occurs at progressively lower pressures as the crack becomes oriented more axially.

To explain the effect of internal pressure on the local buckling of the reinforced cylindrical shells, Vaziri and Estekanchi [27] introduced two mechanisms: (1) the local disturbance of the stress field, in combination with the induced local compressive stress at the crack edges, which tends to decrease the local buckling loads (the dominant effect for axially cracked shells); (2) the stabilizing effect of the internal pressure, which tends to suppress the lower buckling mode of cylindrical shells (the dominant effect for circumferentially cracked shells). Thus, the relative influence of these two mechanisms on the local buckling behavior of cracked cylindrical shells combined with an elastic liner depends on the crack orientation and the internal pressure. For a cracked cylindrical shell with a crack oriented at 30° under relatively low pressure, $\lambda < 2$, the former mechanism associated with the internal pressure dominates the buckling behavior of the shells. By increasing the internal pressure, the buckling load associated with the first local buckling mode of the cylindrical shell reduces considerably (Fig. 10(B)). For a crack oriented at 60° from the circumferential line, the second mechanism dominates the local buckling of the cylindrical shells and the internal pressure reduces the buckling load associated with the first buckling mode of the cracked cylindrical shells.

4. Conclusions

In this paper, we explore the buckling behavior of a cracked thin cylindrical shell reinforced with an elastic liner subjected to both pure axial compression and combined axial compression and internal pressure. We conclude from our study that while elastic reinforcement significantly improves buckling characteristic of the structure compared to the unreinforced case, there are significant differences in buckling behavior depending on crack size, orientation and the material properties of the shell structure and liner. We show that in general, circumferential cracks have less detrimental effect on the mechanical strength of the liner reinforced cylindrical shells than axial cracks. Interestingly, the decrease in buckling strength from a circumferential to an axially oriented crack was not monotonic. From our numerical calculations we find that cracks oriented at about 30° from the circumferential direction showed least decrease in strength, lesser than even the purely circumferential cracks. However, thereafter, buckling strength decreased steadily to reach its minima at the axial direction. Through our extensive parametric studies, we were able to provide a map depicting the state of buckling in global, local or transition zone of buckling depending on the relative thickness, relative stiffness, and the crack orientation. We believe that such transition maps can be a very useful tool in predicting the type of failure. For instance, local buckling failure may not cause a catastrophic failure of the structure but serve as a nucleating site for future interfacial crack propagation between the liner and the shell structure. Finally, we study the effect of internal pressure on the buckling behavior of cracked reinforced cylindrical shells. We find that internal pressure may stabilize against local buckling by suppression at the lower internal pressure zone or may precipitate local buckling of the reinforced cylindrical shells due to stress concentration at higher internal pressure zone depending upon the elastic and geometric properties of the structure.

Acknowledgments

This work has been supported by the Qatar National Research Foundation (QNRF) under Award no. NPRP 09-145-2-061.

References

[1] Farshad M. Design and analysis of shell structures, vol. 16. Springer, Kluwer Academic, Boston; 1992.
[2] Hilburger MW. Buckling and failure of compression-loaded composite laminated shells with cutouts. NASA Langley Research Center; 2007.
[3] Budiansky B, Hutchinson J. Buckling of circular cylindrical shells under axial compression; 1972.
[4] Lord G, Champneys A, Hunt GW. Computation of localized post buckling in long axially compressed cylindrical shells. Philosophical Transactions of the Royal Society of London. Series A: Mathematical, Physical and Engineering Sciences 1997;355(1732):2137–50.
[5] Hutchinson J, Muggeridge D, Tennyson R. Effect of a local axisymmetric imperfection on the buckling behaviorof a circular cylindrical shell under axial compression. AIAA Journal 1971;9(1):48–52.
[6] Barut A, Madenciv E, Britt O, Starnes J. Buckling of a thin, tension-loaded, composite plate with an inclined crack. Engineering Fracture Mechanics 1997;58(3):233–48.
[7] Khamlichi A, Bezzazi M, Limam A. Buckling of elastic cylindrical shells considering the effect of localized axisymmetric imperfections. Thin-Walled Structures 2004;42(7):1035–47.
[8] Hilburger MW, Starnes JH. Effects of imperfections of the buckling response of composite shells. Thin-Walled Structures 2004;42(3):369–97.
[9] Estekanchi H, Vafai A. On the buckling of cylindrical shells with through cracks under axial load. Thin-Walled Structures 1999;35(4):255–74.
[10] Javidruzi M, et al. Vibration, buckling and dynamic stability of cracked cylindrical shells. Thin-Walled Structures 2004;42(1):79–99.
[11] Rajani B, Kleiner Y. Comprehensive review of structural deterioration of water mains: physically based models. Urban Water 2001;3(3):151–64.
[12] Hutchinson JW. Buckling and initial postbuckling behavior of oval cylindrical shells under axial compression. Journal of Applied Mechanics 1968;35(1):66–72.
[13] Hutchinson JW. On the postbuckling behavior of imperfection-sensitive structures in the plastic range. Journal of Applied Mechanics 1972;39(1):155–62.
[14] Koiter W. The effect of axisymmetric imperfections on the buckling of cylindrical shells under axial compression. Proceedings of the Koninklijke Nederlandse Akademie van Wetenschappen 1963:265–79.
[15] Krishnakumar S, Foster C. Axial load capacity of cylindrical shells with local geometric defects. Experimental Mechanics 1991;31(2):104–10.
[16] Li YW, Elishakoff I, Starnes JH. Axial buckling of composite cylindrical shells with periodic thickness variation. Computers & Structures 1995;56(1):65–74.
[17] Li Y-W, et al. Effect of the thickness variation and initial imperfection on buckling of composite cylindrical shells: asymptotic analysis and numerical results by BOSOR4 and PANDA2. International Journal of Solids and Structures 1997;34(28):3755–67.
[18] Dimarogonas AD. Buckling of rings and tubes with longitudinal cracks. Mechanics Research and Communication 1981;8:179–86.
[19] Riks E, Rankin CC, Brogan FA. The buckling behavior of a central crack in a plate under tension. Engineering Fracture Mechanics 1992;43:529–47.
[20] Khedmati MR, Edalat P, Javidruzi M. Sensitivity analysis of the elastic buckling of cracked plate elements under axial compression. Thin-Walled Structures 2009;47:522–36.

[21] Brighenti R. Buckling sensitivity analysis of cracked thin plates under membrane tension or compression loading. Nuclear Engineering and Design 2009:965–80239 2009:965–80.
[22] Athiannan K, Palaninathan R. Buckling of cylindrical shells under transverse shear. Thin-Walled Structures 2004;42:1307–28.
[23] Brighenti R, Carpinteri A. Buckling and fracture behaviour of cracked thin plates under shear loading. International Journal of Materials and Design 2011;32:1347–55.
[24] Alinia MM, Dastfan M. Behaviour of thin steel plate shear walls regarding frame members. Journal of Constructional Steel Research 2006;62:730–8.
[25] El Naschie M. A branching solution for the local buckling of a circumferentially cracked cylindrical shell. International Journal of Mechanical Sciences 1974;16 (10):689–97.
[26] Dyshel' MS. Stability of a cracked cylindrical shell in tension. International Applied Mechanics 1989;25(6):542–8.
[27] Vaziri A, Estekanchi HE. Buckling of cracked cylindrical thin shells under combined internal pressure and axial compression. Thin-Walled Structures 2006;44(2):141–51.
[28] Vaziri A. On the buckling of cracked composite cylindrical shells under axial compression. Composite Structures 2007;80(1):152–8.
[29] Haghpanah Jahromi B, Vaziri A. Instability of cylindrical shells with single and multiple cracks under axial compression. Thin-Walled Structures 2012;54:35–43.
[30] Timoshenko SP, Green JM. Theory of elastic stability. McGraw-Hill Book Co., New York; 1961.
[31] Reddy JN. Mechanics of laminated composite plates and shells: theory and analysis. Boca Raton, FL: CRC Press; 2003.
[32] Rutgerson SE, Bottega WJ. Thermo-elastic buckling of layered shell segments. International journal of solids and structures 2002;39.19:4867–87.